

# Response to ERR comments and recommendations on GMN detector simulations

Eric Fuchey, Andrew Puckett, and Seamus Riordan

July 17, 2017

## 1 Charge Item 5 recommendation: “A complete and realistic simulation of the full detector response, in particular for the HCAL and CDET, is needed.”

A complete and realistic simulation machinery for the full response of the GMN detectors already exists in the form of the *g4sbs* package, and was already used to carry out the simulations that addressed charge item 8 of the ERR (radiation levels and local shielding). In response to the questions raised by the ERR committee regarding the background rates and performance of the SBS detectors including CDET and HCAL, additional studies were carried out since the review to determine the signal-to-background ratios and operating parameters of these detectors under the expected conditions during GMN, and the effects of the background on the detector performance, including the coordinate, energy, and timing resolution of HCAL in particular. The BigBite timing hodoscope was also added to *g4sbs* for completeness, although the background environment in this detector is expected to be relatively quiet since it is shielded by the BigBite preshower calorimeter.

This document will focus in particular on the background rates in HCAL and, to a lesser extent, the CDET, since the BigBite detector backgrounds (excepting the timing hodoscope), were already examined in great detail in addressing charge item 8. Several salient facts about the role of HCAL in the GMN experiment bear repeating here:

1. HCAL is *not* part of the online trigger for the GMN experiment, which will be formed from the BigBite calorimeter signals only.
2. The signals from each of the 288 individual PMTs of HCAL will be read out for each trigger using Flash ADCs and (pipeline?) TDCs. The Flash ADC readout will consist of 6-8 samples at 250 MHz rate within a 24-32 ns window encompassing the main signal.
3. The HCAL signals due to quasi-elastically scattered nucleons have a FWHM of 10-15 ns, which sets the time scale for the readout and the evaluation of the signal-background ratio.
4. CDET is *not* a critical subsystem for the experiment, but is used merely as a redundant cross-check of the neutron and proton identification. It is also not part of the trigger.

The background levels in all the GMN detectors were calculated by throwing a large number ( $N_e \approx 11 \times 10^9$ ) of beam electrons at the LD2 target, simulating “all” physics processes involved in 11 GeV fixed target electron-nucleus scattering, and recording the rates of energy deposition and, as applicable, optical photon detection, in all of the GMN detectors. The geometry of the downstream beamline is described in full detail using the final design. A preliminary geometry of local shielding of the downstream beamline and scattering chamber area to reduce the background rates in the BigBite detectors is also included. The optical properties of HCAL governing the photoelectron yield in response to a given energy deposition in its plastic

scintillator tiles is also fully detailed, including scintillation yields and time constants, refractive indices, wavelength shifter absorption and re-emission spectra, and lightguide geometry. While these properties are well documented and benchmarked against cosmic ray test data from the actual HCAL modules, the signal-to-background ratio estimates presented here can be derived directly from the energy deposition rates in the HCAL scintillator and a separate simulation of the energy deposition by the quasi-elastically scattered nucleons of interest, and do not depend on the details of simulated optical photon production and tracking, which are inherently more uncertain.

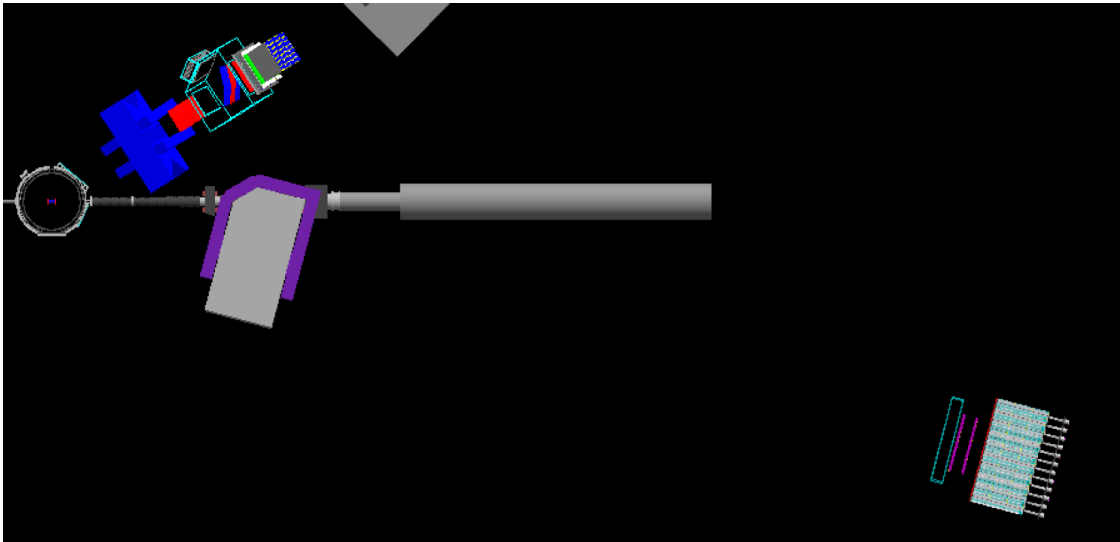


Figure 1: Layout of GMN detectors in *g4sbs*, with latest, fully detailed HCAL geometry, benchmarked against cosmic ray data.

Figure 1 shows the latest GMN layout in *g4sbs* (without beamline shielding). Figure 2 shows a side view of the BigBite detector package illustrating the location of the BigBite hodoscope scintillator paddles.

## 1.1 HCAL analysis

The signal in HCAL is linearly proportional to the energy deposition in the plastic scintillator. Because HCAL is a sampling calorimeter with iron as the passive absorber material and scintillator as the active medium, the sampling fraction is relatively small. The average number of photoelectrons per unit energy deposited is relatively large ( $\approx 3,000$  p.e.'s/GeV), but the PMT signals are subject to large statistical fluctuations due to the small sampling fraction of HCAL and the intrinsic fluctuations in the hadronic shower development at the few-GeV nucleon energies of the GMN experiment. The total background rate of energy deposition in the HCAL scintillator was estimated from the simulation to be  $dE/dt = 6.4 \times 10^7$  MeV/s/module, with module-to-module variations ranging from  $4 \times 10^7$  to  $12 \times 10^7$  MeV/s. Figure 3 shows the total counting rate as a function of threshold; i.e., the minimum total energy deposited in scintillator over the entire HCAL. Figure 3 also shows the distribution of the total energy deposited in HCAL within a 50-ns window, which is about twice the width of the expected window for charge integration of the PMT pulses of the quasi-elastic nucleon signal. Note that the average energy deposition rate per module would be obtained by dividing the rates shown in Fig. 3 by the total number (288) of modules. HCAL is subject to a very high rate of very low-energy background. The average HCAL hit rate for a threshold of 11 MeV (corresponding to roughly 2% of the average quasi-elastic nucleon signal), is about 500 kHz, with module-to-module variations ranging from 200 kHz-1 MHz. The FWHM of the HCAL PMT signal is approximately 10-15 ns, so the relevant time window for charge integration of the HCAL signal is (conservatively) 25-30 ns. On this time scale,

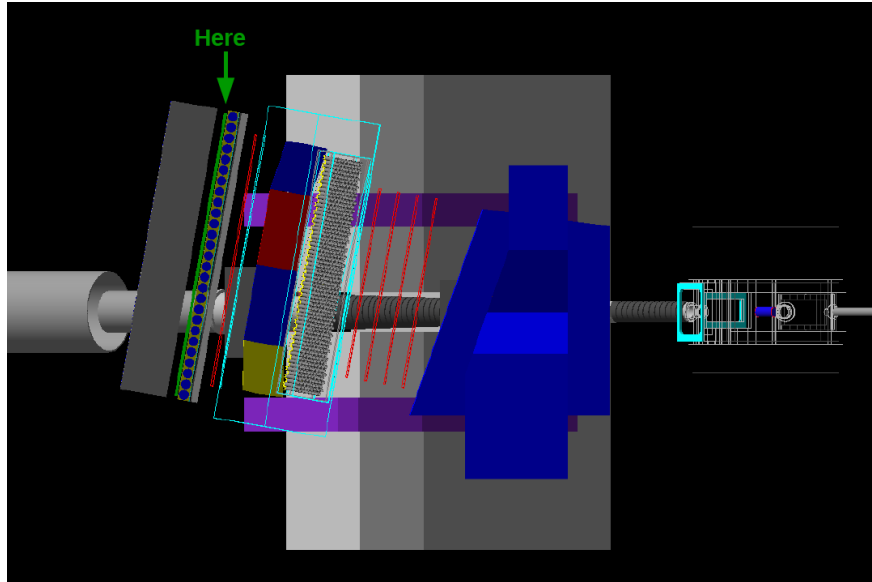


Figure 2: Layout of BigBite detectors in  $g4sbs$ , with the geometry of the new BigBite timing hodoscope added (see arrow “Here”).

the maximum observed hit rate of 1 MHz/module for an 11 MeV threshold corresponds to a roughly 3% PMT occupancy. The higher-rate, lower-energy background manifests as a baseline shift of the signal and a broadening of the “pedestal” noise. The very low-energy background rate also contributes to the PMT anode current, when the operating gain of the PMT, the analog chain between the PMT and the readout electronics, and the signal-to-background ratio are taken into account.

Figure 4 shows the distribution of signals produced in HCAL by quasi-elastically scattered nucleons at  $Q^2 = 13.5 \text{ GeV}^2$ , as well as the distribution of the hit multiplicity in HCAL per quasi-elastic nucleon, for a threshold of 2% of the average total energy deposition, or 11.2 MeV. The total energy deposition has a broad peak at about 560 MeV with a standard deviation of about 120 MeV, while the maximum energy deposition in a single module peaks at about 210 MeV, with a standard deviation of about 100 MeV. On average, the hadronic shower of quasi-elastic nucleons at the highest  $Q^2$  is spread among 7.2 modules, with a standard deviation of 2.3 modules. Close to 100% of the showers are contained within 15 modules for a threshold of 2% of the average total energy deposition. This implies that the *average* energy deposition per module in the hadronic shower of a quasi-elastically scattered nucleon is about 78 MeV. For a 30-ns window for charge integration of the PMT pulse, the *average* signal in a single block of 78 MeV is to be compared to an *average* background energy deposition of about 1.9 MeV, with fluctuations at the level of 0.24 MeV. The average signal-to-background ratio for a conservative timing window for the signal is about 40. The peak signal-to-background ratio would be approximately twice the average, or about 80. A Monte Carlo simulation of the effect of the low-energy background on the efficiency, energy and coordinate reconstruction found no significant effects on either the efficiency or the energy and coordinate resolution for quasi-elastic nucleons.

The operating gain of the HCAL PMTs will be adjusted such that the maximal voltage amplitude of the PMT signal is about 200 mV, corresponding to an integrated charge of approximately 60 pC. The raw PMT signal will be fed to a 10X amplifier at the front end prior to transmission down a long ( $\approx 100\text{-m}$ ) cable to the readout electronics. The amplifier at the front end allows the PMTs to be operated at relatively low gain, which reduces the anode current, leading to improved stability and longer lifetime. The largest expected signal from a single PMT corresponds to roughly 500 MeV of energy deposition. This implies that

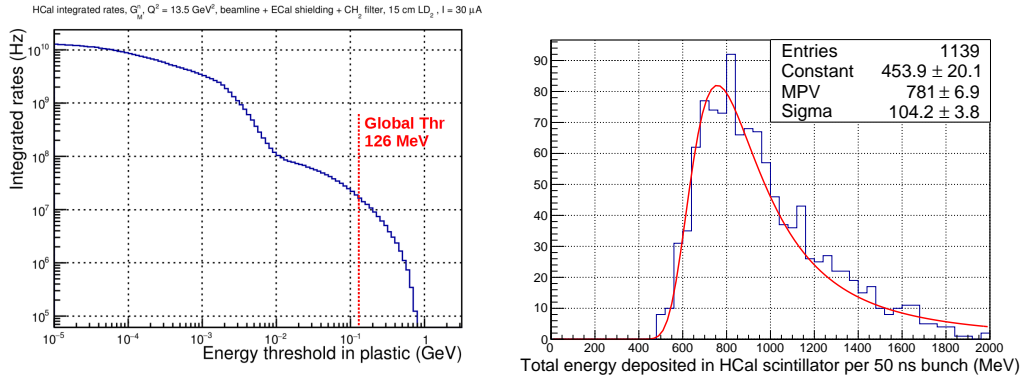


Figure 3: Left: Total counting rate as a function of the threshold for energy deposition in the HCal scintillator for the  $Q^2 = 13.5 \text{ GeV}^2$  setting of GMN, integrated over the entire HCal. The average rate per channel/PMT would be obtained by dividing the rate by the total number of modules (288). The vertical line at 126 MeV represents the approximate threshold applied to the signal. The average energy deposition in the scintillator by the quasi-elastically scattered nucleons of interest is approximately 560 MeV at this  $Q^2$ . Right: Distribution of the total energy deposited in HCal during a 50 ns window, for approximately 1,100 independent simulated 50-ns intervals of beam on target. The implied average energy deposition per module during a 50 ns window is  $2.7 \text{ (MPV)} \pm 0.4 \text{ (Sigma)} \text{ MeV}$ .

the expected operating gain of the PMT corresponds to about 120 fC of integrated charge per MeV of energy deposited. When multiplied by the average background energy deposition rate of  $6.4 \times 10^7 \text{ MeV/s/module}$ , the corresponding average PMT anode current would be  $7.7 \mu\text{A}$ , which is a relatively high, but tolerable operating current. For reference, the maximum continuous anode current rating for the Photonis XP2262 PMTs that will be used for HCal is  $200 \mu\text{A}$ . Assuming a photoelectron yield of 3,000/GeV, the implied operating gain is  $2 \times 10^5$ , which is a relatively comfortable operating condition for the XP2262.

## 1.2 CDET Analysis

The layout of the coordinate detector (CDET) for the simulation is shown in Fig. 1. While the final layout will likely involve horizontal staggering to cover as much of the HCal acceptance as possible, for the estimation of signal-to-background ratios, the CDET was stacked as two planes with 100% overlap in terms of active area, and the results presented here refer to this configuration. The purpose of the CDET in GMN is to provide a redundant cross check of the particle identification. It is sensitive to protons and insensitive to neutrons, to a good approximation. The average background energy deposition rate in a single strip of the CDET scintillator is estimated from the simulation to be  $8 \times 10^6 \text{ MeV/s}$ . The quasi-elastic protons passing through CDET typically deposit about 7 MeV in one scintillator strip, as shown in Figure 5. The maximum energy deposition in a single strip by quasi-elastic nucleons extends to about 150 MeV with low probability, however, 97% of quasi-elastic protons deposit less than 70 MeV or about 10 times the minimum-ionizing peak. According to current plans, only timing information will be read out for the CDET, using the NINO amplifier/discriminator card with a fixed discriminator threshold that produces an output LVDS logic pulse with a width of 10 ns plus the time over threshold. The expected number of photoelectrons for typical signals (those characteristic of the main, minimum-ionization peak) is about 40, based on bench tests of the CDET modules. The nominal operating gain of the CDET maPMTs is  $3 \times 10^5$ . Assuming 40 photoelectrons for a typical signal at a gain of  $3 \times 10^5$ , the typical PMT pulse will have a charge of about 1.9 pC, with a duration of about 10 ns. The expected background hit rates in the CDET for a threshold of 5.5 MeV are at the level of 0.1-0.3 MHz, and pose no significant difficulties for readout or offline analysis. Using a conservative estimate of a 10 ns window for the main signal, the average background energy deposition during this window is 0.08

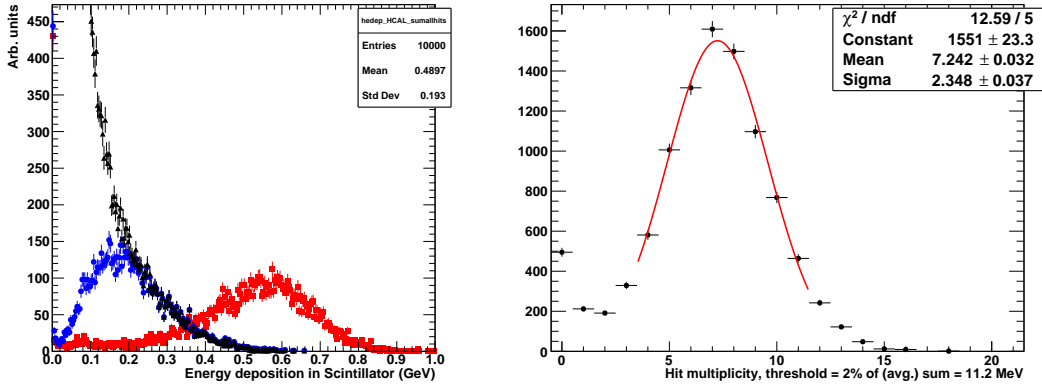


Figure 4: Left: Energy deposition in HCAL scintillator by quasi-elastically scattered nucleons for  $Q^2 = 13.5$   $\text{GeV}^2$ . Red squares show the total sum over all hits in all modules, blue circles show the distribution of the hit with the largest energy deposition, and black triangles show the distribution of all hits. Right: Hit multiplicity in HCAL per quasi-elastic nucleon, for a threshold of 11.2 MeV, or 2% of the average total energy deposit.

MeV. The average (peak) signal-to-background ratio for the CDET, then, is about 88 (176). The average (per-pixel) maPMT anode current corresponding to the background energy deposition rate in CDET under these assumptions is about  $2.2 \mu\text{A}$ .

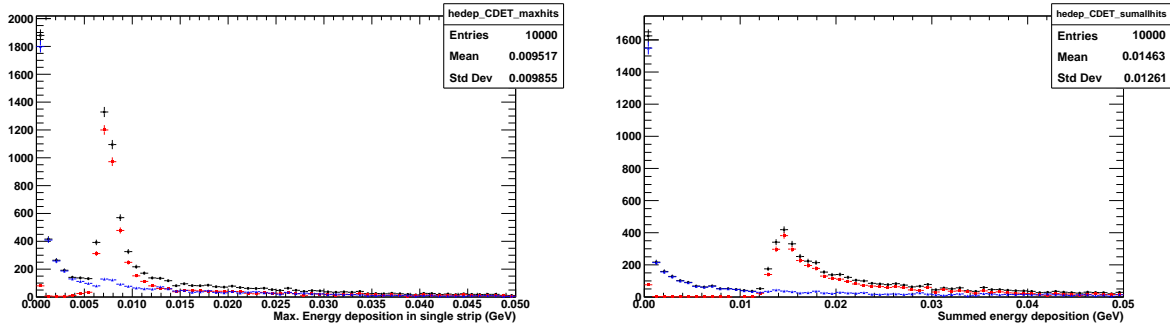


Figure 5: Energy deposition by quasi-elastically scattered nucleons in CDET for the  $13.5 \text{ GeV}^2$  setting of GMN. Left: Maximum energy deposition in a single strip, for all nucleons (black circles), protons (red squares), and neutrons (blue triangles). The threshold used to estimate the hit rates and compute the hit multiplicities and signal/background ratios is 5.5 MeV.

### 1.3 BigBite Hodoscope Analysis

The BigBite hodoscope consists of 90 scintillator paddles, each with PMTs at both ends. The scintillators are wrapped in non-reflective black Tedlar, such that only the totally internally reflected light reaches the PMT. Figure 6 shows the distribution of energy deposition in the BigBite timing hodoscope by quasi-elastically scattered electrons, for the  $13.5 \text{ GeV}^2$  kinematics. The average total energy deposition in the hodoscope is about 100 MeV, while the average energy deposition in the scintillator paddle with the largest signal is

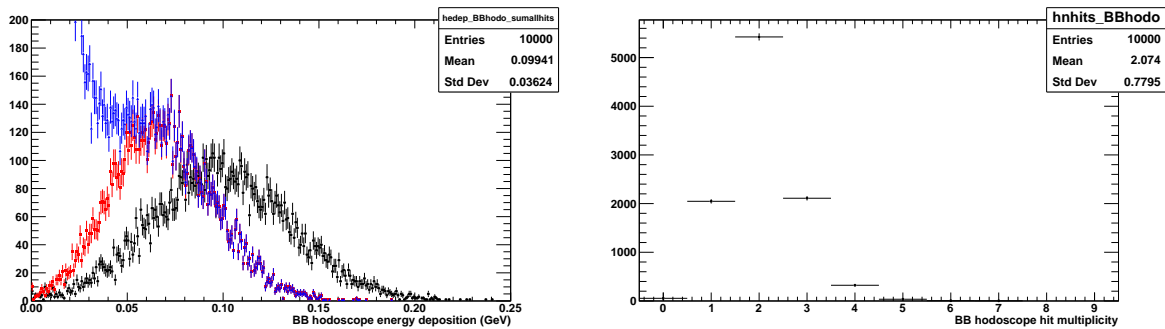


Figure 6: Left: Energy deposition in the BigBite timing hodoscope for quasi-elastically scattered electrons at  $Q^2 = 13.5 \text{ GeV}^2$ . Black circles show the sum total of all energy depositions in the BigBite hodoscope. Red squares show the maximum energy deposition in a single scintillator bar. Blue triangles show the distribution of energy deposition for all hits. Right: hit multiplicity in the BigBite timing hodoscope per quasi-elastic electron, for a threshold of 8 MeV.

about 75 MeV. Note that the energy deposition in the hodoscope is greater than would be expected for minimum-ionizing particles because it is located between the preshower and shower detectors, and therefore detects a significant number of low-energy charged secondaries produced in the electromagnetic cascade. A high efficiency for the quasi-elastic electrons is achieved with a threshold of 8 MeV. The average hit rate per channel in the timing hodoscope for this threshold is 300 kHz. For a 10-ns window for the main signal, the implied average channel occupancy is about 0.3%. The average energy deposition rate per channel of the BigBite timing hodoscope is  $1.2 \times 10^7 \text{ MeV/s}$ . The average background energy deposition in a 10-ns timing window is 0.12 MeV. Compared to the average energy deposition of 75 MeV in the hodoscope paddle with the largest signal, the average signal-to-background ratio is about 625. It is reasonable to assume that on average, the total energy deposit will be divided roughly equally between the two PMTs, although in practice, the PMTs closer to the beam will likely have somewhat higher background rates and anode currents. Bench tests with cosmic rays indicate that the amplitude of the PMT signal varies by roughly a factor of two as a function of the hit position along the paddle, while the average amplitude of the two PMT signals is approximately 11% lower at the middle of the bar than at either end. Based on these tests, the maximum signal amplitude is estimated to be about 1.4 times the average signal amplitude. The NINO front-end card that will be used for the hodoscope is sensitive to small-amplitude input signals, so it is likely that the operating gain of the PMT will be such that the voltage amplitude corresponding to the maximal signal is not more than about 200 mV. From Figure 6, the maximal energy deposition in a single paddle is about 150 MeV. Each PMT receives an average of approximately half the total charge (photoelectron yield) due to this maximal signal. In order to give a maximal signal around 200 mV, the average signal corresponding to 150 MeV energy deposition should be about 140 mV. Assuming a 10-ns signal duration, an average amplitude of half the peak amplitude, and 50-Ohm impedance, the average PMT pulse charge for 150 MeV of energy deposition will be about 28 pC. The implied average anode current corresponding to the background energy deposition rate of  $1.2 \times 10^7 \text{ MeV/s}$  is  $2.2 \mu\text{A}$ . The ET9125 PMTs for the BigBite timing hodoscope have a maximum current rating of  $100 \mu\text{A}$ .

#### 1.4 BigBite Shower/Preshower Analysis

Figure 7 shows the energy deposition and hit multiplicities in the BigBite pre-shower calorimeter for quasi-elastically scattered electrons at  $Q^2 = 13.5 \text{ GeV}^2$ . The average total energy deposition per QE electron is about 750 MeV. The energy deposition in the block with the largest signal exhibits a similar distribution to the total energy, averaging about 680 MeV. The total signal in the pre-shower is contained in one or

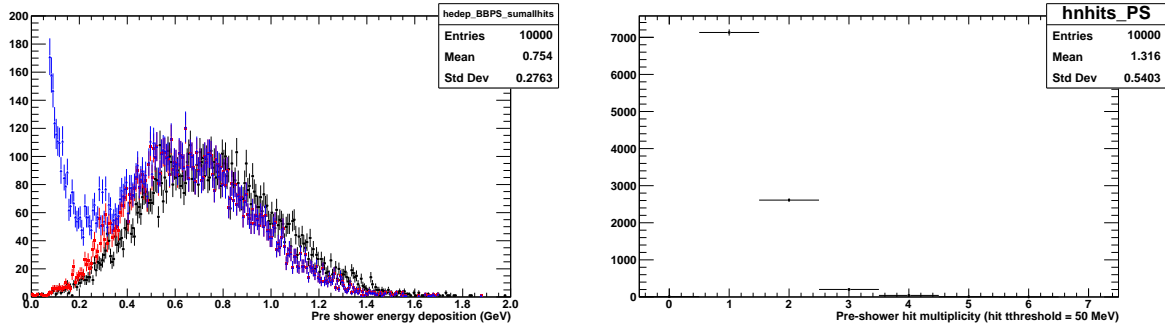


Figure 7: Left: Pre-shower energy deposition for QE electrons. Black circles show the sum total energy deposition per quasi-elastic electron in the entire preshower. Red squares show the energy deposition in the pre-shower block with the largest signal. Blue triangles show the energy deposition for all pre-shower hits. Right: Hit multiplicity in the pre-shower per quasi-elastic electron, for a hit threshold of 50 MeV.

two blocks in the vast majority of events, as the right panel of Fig. 7 shows. The average hit multiplicity in the preshower per quasi-elastic electron is 1.3 for a threshold of 50 MeV. The average hit rate in the preshower for a hit threshold of 50 MeV, corresponding to an efficiency greater than 99% for quasi-elastic electrons, is 1.1 MHz. For a conservative, 30-ns window for the signal, the average channel occupancy is 3.3%. The background energy deposition rate per block in the preshower is  $2.5 \times 10^8$  MeV/s. The background energy deposition in a 30-ns window is 7.6 MeV. Compared to the average quasi-elastic signal of 680 MeV, divided by the average hit multiplicity of 1.3, the average signal-to-background ratio is about 69. The peak signal-to-background ratio would be roughly twice as high, or about 138.

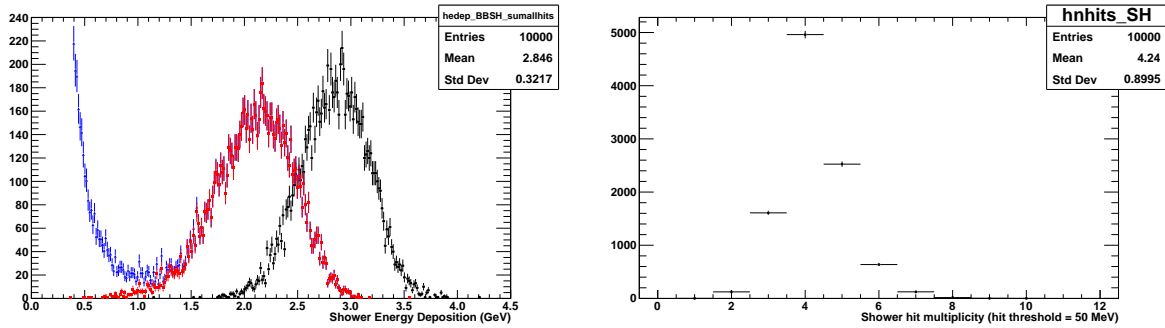


Figure 8: Left: Shower energy deposition for QE electrons. Black circles show the total energy deposition in the entire shower calorimeter per QE electron. Red squares show the energy deposition in the shower block with the largest signal. Blue triangles show the energy deposition for all shower hits. Right: Hit multiplicity per QE electron in the shower, for a hit threshold of 56 MeV, or about 2% of the average total energy deposition.

Figure 8 shows the energy deposition and hit multiplicities in the BigBite shower calorimeter for quasi-elastically scattered electrons at  $Q^2 = 13.5$  GeV<sup>2</sup>. The average total energy deposition per QE electron is about 2.8 GeV. The maximum energy deposition in a single block averages about 2.1 GeV. For a 50 MeV threshold, the average hit multiplicity per quasi-elastic electron is 4.2. The average background hit rate per channel in the shower is 374 kHz. For a 30-ns signal duration, the implied average channel occupancy

is 1.1%. The background energy deposition rate in the shower is  $9.4 \times 10^7$  MeV/s. The implied average signal-to-background ratio from the energy deposition rate is 177.

For the preshower and shower detectors, in contrast to the scintillation detectors, the photoelectron yield is not linear with energy deposition down to arbitrarily small energy depositions, because the production of optical photons is subject to the Cherenkov radiation threshold, which is approximately 0.7 MeV (momentum) or 0.3 MeV (kinetic energy) for electrons in lead-glass. Below this minimum energy, no optical photons are produced. The average photoelectron yield according to the optical properties of lead glass and PMT quantum efficiency in the simulation is about 1,200 ph.e./GeV for the preshower, and about 1,700 ph.e./GeV for the shower. These are likely overestimates, and thus represent a worst-case scenario in terms of PMT anode current for a given operating gain. The estimated average background photoelectron rate for the preshower (shower) is  $3.4 \times 10^8$  ( $1.8 \times 10^8$ ) p.e.'s/s. These background rates correspond to average PMT anode currents of  $5.4 \mu\text{A}$  ( $2.9 \mu\text{A}$ ) for an operating gain of  $10^5$ . The average signal-to-background ratios estimated directly from the simulated photoelectron yields (as opposed to the energy deposition rates) are 133 (234) for the preshower (shower) for a 30-ns signal duration. The maximum signal amplitude for the preshower (shower) signals for a PMT gain of  $10^5$  is 93 (286) mV.

## 2 Summary of performance for HCAL, CDET, BigBite timing hodoscope, and BigBite calorimeter

Table 1: Summary of detector performance at  $Q^2 = 13.5 \text{ GeV}^2$  in terms of signal-background ratios, PMT anode currents, and occupancies. See text for details.

Quantity	HCAL	CDET	BB Hodoscope	BB Preshower	BB Shower
$\langle E_{dep}^{QE} \rangle$ , sum over all channels (MeV)	560	7.2	100	750	2,800
$\langle E_{dep}^{QE} \rangle$ , channel w/ max. signal (MeV)	210	7.2	75	680	2,100
Max. $E_{dep}^{QE}$ , single channel (MeV)	500	72	150	1,600	3,200
$\langle N_{hits}^{QE} \rangle$	7.2	1 (2)	2.1	1.3	4.2
Channel occupancy (%)	3	0.3	0.3	3.3	1.1
Background $\frac{dE_{dep}}{dt}$ (MeV/s)	$6.4 \times 10^7$	$8 \times 10^6$	$1.2 \times 10^7$	$2.5 \times 10^8$	$9.4 \times 10^7$
Background $\frac{dN_{phe}}{dt}$ (ph.e./s)	$2.3 \times 10^8$	$4.4 \times 10^7$	N/A	$3.4 \times 10^8$	$1.8 \times 10^8$
PMT gain (typical)	$2 \times 10^5$	$3 \times 10^5$	$10^4$ - $10^5$	$10^5$	$10^5$
PMT anode current ( $\mu\text{A}$ )	7.7	2.2	2.2	5.4	2.9
Signal duration (ns)	30	10	10	30	30
Avg. S/B ratio from $E_{dep}$	40	88	625	N/A	N/A
Avg. S/B ratio from $N_{phe}$	N/A	N/A	N/A	133	234
Avg. (max) signal amplitude (mV)	84 (200)	19 (190)	140 (200)	42 (93)	192 (286)

Table 1 summarizes the results of the full simulation of the detector response to both the signal and the background in GMN at  $Q^2 = 13.5 \text{ GeV}^2$ , for all GMN detectors *other than* GRINCH and the BigBite GEMs, which were addressed in detail in our original response to charge item 8 of the ERR. The average hit multiplicity in CDET is for quasi-elastic *protons*, and is 2 in areas of overlap between the two planes

of CDET modules (1 outside). In first approximation, the CDET is not sensitive to neutrons. A reliable estimate of the photoelectron yield for the BigBite timing hodoscope is pending. Hit rates and channel occupancies are estimated using the highest threshold that gives  $> 99\%$  efficiency for the quasi-elastic signal. Signal-to-background ratios for the scintillation-based detectors are estimated from the background energy deposition rates and the signal duration and energy deposition. Specifically, the average total energy deposition by the particles of interest is divided by the average hit multiplicity per quasi-elastic electron/nucleon to obtain an effect average signal-to-background ratio. For the Cherenkov-based detectors (preshower and shower calorimeters), the signal-to-background ratios are estimated directly from the simulated photoelectron yields. In all cases, the signal-to-background ratios are high, and the PMT anode currents due to the low-energy background are in the 1-10  $\mu\text{A}$  range under reasonable assumptions on operating gain. These anode currents are relatively high, but entirely tolerable with considerable safety margins relative to the maximum continuous anode current ratings of the PMTs that will be used. Under these conditions, no significant aging effects or rate effects on the gain/linearity are expected, and the PMT gains can be lowered, in principle, if the photoelectron yields are higher than estimated.